

## Energy saving procedures for fishing vessels by means of numerical optimization of hull resistance

Tomasz Abramowski<sup>✉</sup>, Karol Sugalski

Maritime University of Szczecin  
1-2 Wały Chrobrego St., 70-500 Szczecin, Poland  
e-mail: {t.abramowski; k.sugalski}@am.szczecin.pl  
<sup>✉</sup> corresponding author

**Key words:** CFD, hull shape optimization, fishing boat, hull resistance, OpenFoam, simulation

### Abstract

This paper presents the general method for hull shape optimization of fishing boats with the objective of reducing resistance. In particular, it presents an example of the results of the application of resistance-reducing devices such as the ducktail, the cylindrical bulb and the streamlined bulbous bow. The resistance was determined using computational fluid dynamics (CFD). For the purpose of flow simulation, the *OpenFoam* system, distributed under an open source license, was used. The turbulent, unsteady flow with free surface liquid around the analyzed hulls was computed and investigated for potential resistance reduction. Ultimately, the calculation results were generalized by the parameterization of dimensionless geometric variables for the shape of a bulbous bow and were given in a form suitable for practical application in the hull design process.

### Introduction

The objective of this paper is to present a procedure for optimization of hull shape with the objective of reducing the energy requirements of the propulsion systems of representative fishing vessels operated within the Polish fishing fleet. The research was carried out as part of the EU project *Conducting expert studies on plans for restructuring and modernization of the Polish fishing fleet, based on selected fishing vessels in order to reduce the negative impact on marine ecosystems*, funded by the European Maritime and Fisheries Fund.

Reducing the energy requirements of the propulsion system was achieved through modifications that can potentially result in minimization of the hull resistance and, consequently, the effective power consumption (Fyson, 1985; Gulbrandsen, 2012). These are significant technical characteristics of the fishing boats that have a considerable impact on the overall energy requirements of the fishing vessels during their operation.

The subjects of the optimization process are typical fishing vessels of types: K15, STOREM4, B25, KB21, B410, B403, B280, B275 and B368. Their principal characteristics are given in Table 1. Only select examples of calculations have been presented in this paper; nevertheless, the described synthetic procedure and generalization of the results offer potential for practical application. The detailed technical characteristics of the fishing vessels studied can be found in the literature (Foltyn, 1978; Blady, 2002).

The proposed procedure was separated into partial tasks; their completion, and the detailed results, allowed us to formulate general conclusions related to the modification of the shape of the boats' hulls. Some of the tasks were ancillary such as the recovery of the technical documentation for fishing boats already in operation for several decades; their accomplishment was however necessary for the analysis and served to determine and manage the input data, the range of variation of parameters, boundary conditions and design variables.

**Table 1. Summary of all fishing vessels' principal characteristics that were the subject of investigations**

| Description | $L_c$ [m] | $L_{pp}$ [m] | $B$ [m] | $T_{av}$ [m] | $H$ [m] | $L/B$ [-] | $B/T$ [-] | $V$ [kts] | $F_n$ [-] |
|-------------|-----------|--------------|---------|--------------|---------|-----------|-----------|-----------|-----------|
| 15          | 17.8      | 16.9         | 5.0     | 2.0          | 2.4     | 3.4       | 2.5       | 8.0       | 0.319     |
| STOREM4     | 17.5      | 16.2         | 5.3     | 2.5          | 2.7     | 3.1       | 2.1       | 8.5       | 0.346     |
| B25         | 24.6      | 21.9         | 6.6     | 2.3          | 3.4     | 3.3       | 2.9       | 8.0       | 0.351     |
| KB21        | 21.0      | 19.0         | 6.0     | 2.2          | 3.0     | 3.2       | 2.7       | 10.0      | 0.376     |
| B410        | 25.8      | 23.0         | 7.2     | 2.7          | 3.5     | 3.2       | 2.7       | 11.0      | 0.376     |
| B403        | 25.8      | 23.0         | 7.2     | 2.7          | 3.5     | 3.2       | 2.7       | 11.0      | 0.376     |
| B280        | 26.8      | 23.5         | 7.4     | 3.0          | 3.7     | 3.2       | 2.5       | 10.0      | 0.338     |
| B275        | 29.8      | 26.4         | 8.2     | 3.2          | 6.2     | 3.2       | 2.5       | 10.7      | 0.342     |
| B368        | 17.6      | 15.0         | 5.2     | 2.0          | 2.4     | 2.9       | 2.6       | 9.0       | 0.381     |

Similar problems related to the application of computational fluid dynamics for optimization of propulsion characteristics of ships and general optimization of marine vessels have been the subject of previous discussion (Peri, Rossetti & Campana, 2001; Jacquin et al., 2002; Abramowski, Szelangiewicz, & Żelazny, 2010; Cepowski, 2010; Szelangiewicz, Abramowski & Żelazny, 2010; Abramowski, 2013). The calm water resistance is a subject of consideration in the presented research. Further information on the behavior of ships and their resistance characteristics in waves can also be found (Cepowski, 2009).

## The general procedure and steps

The entire optimization procedure was formally separated into the following tasks:

I. Analysis of the operational performance characteristics of the fishing vessels and their geometrical properties

Identification of important characteristics for the operating conditions of fishing vessels

Analysis of the existing technical documentation with regard to the operating conditions

Identification of geometric parameters essential for optimization tasks

II. Preparation of the digital geometry of hulls of fishing boats suitable for manipulations

Digitization of existing blueprints of sections, waterlines and buttocks

Development of 3D surfaces representing hull geometries

Definition of sets of design modifications for numerical flow analysis

III. Running flow simulations for the determination of hull resistance and effective power

Selection of numerical methods and physical models

Construction of numerical grids and calculation domains surrounding the hulls

Executing simulation runs, results analysis, post-processing

IV. Determination of the propulsion power

Numerical grid reconstruction for wake analysis

Wake calculation

Calculation of propulsion factors, thrust deduction and propulsion power, propeller redesign

V. Design proposals for hull shape and devices to reduce effective power

Identification of geometrical constraints

Development of detailed designs

Development of numerical surfaces and final proposals for geometries

VI. Generalization of the research work results, final parameterization of the proposed changes for all fishing vessels.

Each research step listed above was supposed to provide a design solution, information or constraints on further steps of the optimization process. The deliverables are summarized in Table 2. This paper discusses chosen results and conclusions of stages I, II, III, V and VI from the above.

**Table 2. Description of the deliverables for the research tasks**

| Research task | Deliverables  |
|---------------|---|
| I             | Set of geometric variables and constraints for optimization process             |
| II            | Digital form of hull surfaces subject to further manipulations and optimization |
| III           | Bare hull resistance values and effective power                                 |
| IV            | Propulsion power factors  |
| V             | Final results of geometrical changes given in digital form                      |
| VI            | Parameterized data inputs for the hull shape design                             |

## Digital description and geometry developments

Prior to numerical modeling of flow using computational fluid dynamics, the three-dimensional CAD model should be generated which will be later

used to build the computational domain. In the present study it was necessary to develop models according to the documentation supplied in the form of the blueprints (for boats B25 and B280) and the design documentation of individual frame structures (construction drawings, e.g. fishing vessels of the B410 series) and general arrangements (Foltyn, 1978). The objectives are as follows:

1. Digitization of available blueprinted drawings in the form of bodylines and construction sections;
2. Development of three-dimensional surfaces representing a hull shape.

Development of three-dimensional surfaces, was completed using functions available in computer programs with implemented B-Spline and NURBS algorithms developed for this purpose. Digital forms of the shapes of the hulls are based on providing coordinates (in the adopted system) of an adequate number of points on the surface of the hull to ensure geometries are generated with sufficient accuracy. This is particularly important when using the so-called computer aided and analysis group of systems CAx (CADesign, CAManufacturing, CAEngineering), including numerical methods used in the analysis of hydrodynamics phenomena occurring around the hull (boundary element method and finite volume method) or mechanical strength analysis (finite element method).

Due to the complex shape of a hull, it is difficult to describe the entire surface using just one analytical expression. Therefore, the surface of the hull is divided, by boundary lines, into smaller components called patches which eases analytical description.

The smaller patches can be further divided and patches in the bow region, side region, deck, etc. can be defined.

The symmetry plane projection, of a certain patch denoted by index  $k$  creates sub-region  $D_k$  such that the bonding of all sub-regions gives a region  $D$ . If the shape of a patch is described by function  $y_k = f_k(x, z)$ ,  $\{x, z\} \in D_k$ , the entire shape of a hull can be explicitly expressed by the following sum of the functions:

$$y = \sum_k f_k(x, z) \kappa_k(x, z) \quad (1)$$

where:  $\kappa_k = (x, z)$  – characteristic function of a patch, expressed as follows:

$$\kappa_k = \begin{cases} 1 & \text{for } (x, z) \in D_k \\ 0 & \text{for } (x, z) \notin D_k \end{cases} \quad (2)$$

Function  $y = f(x, z)$  is a spline function merged along boundaries of neighboring patches such that the smoothness and convexity of a hull is ensured. The division of a hull's surface into a number of patches allows for the local modification of the geometry without influencing that of neighboring regions.

The curvature of B-Spline is defined by the broken curve of control points and respectively NURBS surfaces are defined by the 3D mesh of control points. The NURBS surface manipulation and modification can be performed in a straightforward way since each control point affects the shape to a limited extent. B-Splines and NURBS surfaces have the following properties:

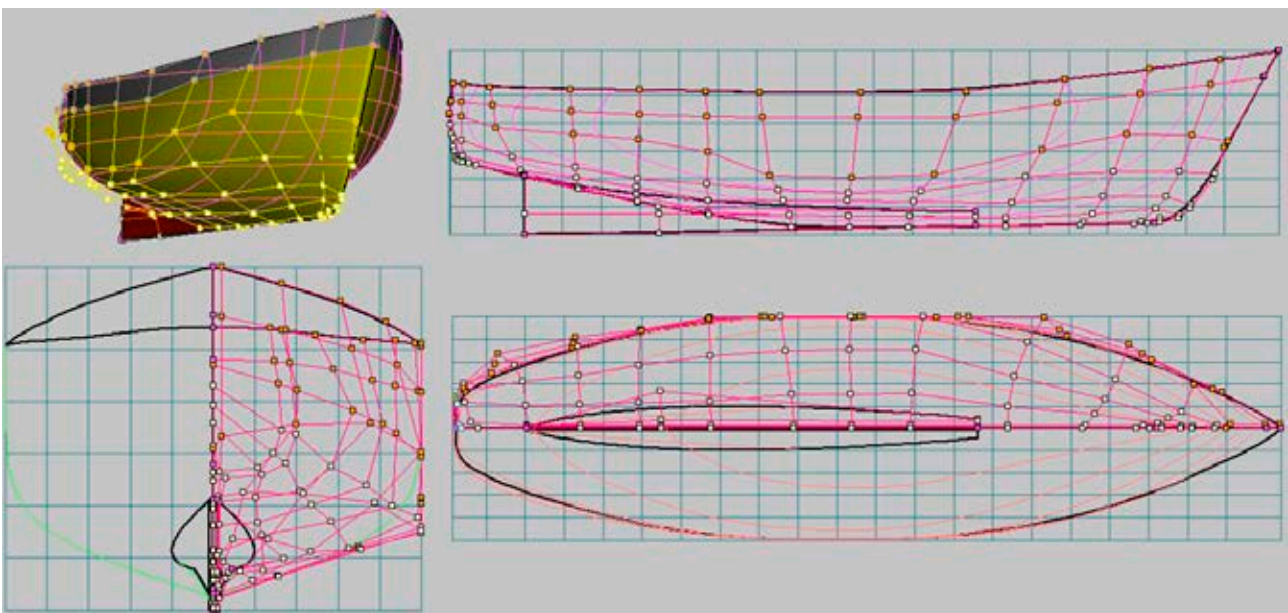


Figure 1. Example of definition of hull surface by the mesh of NURBS control points, B25 fishing boat

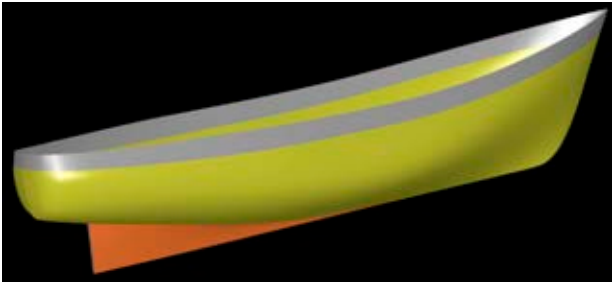
- control points can be placed arbitrarily;
- in the case of NURBS surfaces, the control points are non-uniform which means that a different weight can be assigned to any and each of the control points.

The value of the weight influences the shape (e.g. higher values attract the surface locally); therefore, a change in the value of the weight of a control point can change the curvature without the necessity of changing the control point position.

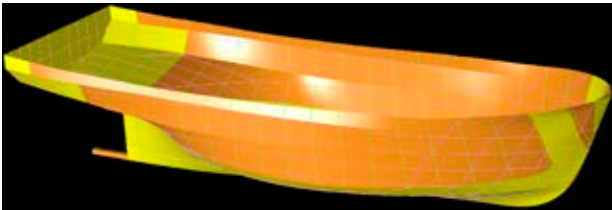
An example of a hull surface defined by a mesh of control points is given in Figure 1. In accordance with the research program, the NURBS definitions for all vessels were developed based on the available documentation. In the latter steps, the shapes were subjected to modification with the aim of generating less resistance and reducing effective power requirement.

Examples of the renderings of representative hull designs are given in Figure 2. The next step is to numerically represent the geometries of the

a)



b)



c)

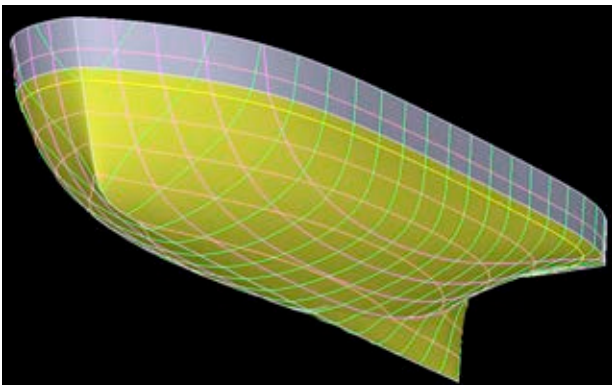


Figure 2. a) rendering of developed surfaces of B25 fishing vessel, b) the shape of B280 fishing vessel, c) the shape of B410 fishing vessel

hull shapes prior to further analysis of propulsion properties.

### Method assumed for flow simulation

To perform the calculations described below, the *OpenFoam* system, on an open source license was used. The governing equations for the flow modeling were the Reynolds equations, RANSE (RANSE – Reynolds-averaged Navier-Stokes equations). For the unsteady, turbulent and incompressible flow case, the equations have the following form in tensor notation:

$$\begin{aligned} \rho \frac{\partial U_i}{\partial t} + \rho U_j \frac{\partial U_i}{\partial x_j} = \\ = \rho F_i - \frac{\partial P}{\partial x_i} + \mu \left( \frac{\partial^2 U_i}{\partial x_j \partial x_j} \right) - \rho \left( \frac{\partial \overline{u'_i u'_j}}{\partial x_j} \right) \end{aligned} \quad (3)$$

where:

$U_{ij}$  –  $U$  vector components of averaged flow velocities,

$P$  – pressure,

$\mu$  – dynamic viscosity,

$u'$  – fluctuation parts of velocities,

$F_i$  – mass forces.

Since the closed control region of the flow is always considered in the simulation, the continuity equation must be fulfilled, for the considered case:

$$\frac{\partial u}{\partial x} + \frac{\partial v}{\partial y} + \frac{\partial w}{\partial z} = 0 \quad (4)$$

Equations (3) and (4) are the system of coupled equations of averaged, incompressible turbulent fluid flow. There are 10 unknowns to be solved: three components of the velocity vector  $[U]$ , the pressure  $P$  and additionally six derivatives of the velocity fluctuation parts, called the turbulent stress tensor or Reynolds stress tensor  $R_{ij}$ . This arrangement of equations does not create a closed system. This is due to the introduction of a speed averaging procedure that eliminates the turbulent fluctuations of the Navier-Stokes equations but at the same time introduces additional unknowns in the form of the Reynolds stress tensor. In this case, the RANS equation should be supplemented with additional equations coupling turbulent stress tensor velocities averaged over time. For this purpose, the two-equation turbulence model  $k-\varepsilon$  was applied. The defined objective of optimization requires proper modeling of free surface effects, which was ensured here by the volume of fluid method, unlike the problems presented by Abramowski

(Abramowski, 2005) where free surface effects could be neglected and the water-air boundary could be modelled as a rigid surface.

The *OpenFoam* solver (OpenCFD Ltd ESI Group, 2016) used in the research is based on the discretization of equations using finite volume method of discretization. The finite volume method is the method most commonly used to solve problems of fluid mechanics, in particular for incompressible, turbulent cases. Due to the editorial restrictions of the journal it is not possible to present here a complete description of the model; further details relating to the procedure of modeling flows by means of computational fluid dynamics can be found in works by Peyret & Taylor (Peyret & Taylor, 1983) and Bertram (Bertram, 2000).

For the meshing procedure of the domains, the native sub-programs, such as *blockMesh* and *snappyHexMesh*, implemented in *OpenFoam* were applied. These programs allow grid generation for complex geometries and simultaneous grid refinement in critical areas like sharp corners and free surface regions. Adequately fine grid arrangement in the regions where a free surface is expected to occur and change its coordinates, as is presented in this research, is essential for the proper modeling of wave resistance.

*BlockMesh* is used to prepare a basic grid, which is the background for the target geometry imported from CAD software. *SnappyHexMesh* creates a grid consisting of unstructured grid elements, though it relies on the presence of a previously created simple domain geometry. It usually has a rectangular shape with domain dimensions already defined and the geometry of the target object around which the flow is to be computed in *STL* format (stereo\_lithography). The *STL* format is one of the basic formats for file import/export operations between various programs for graphic design. The prevailing shape of computational cells in the *OpenFOAM* system is hexagonal. The process of grid generation begins by creating a grid background and inserting it into the *snappyHexMesh* module, the program then starts making the grid background denser along the edge of the geometry of the object in accordance with the degree of grid accuracy specified by the user. The next step is to remove redundant cells from the user-defined spaces within and outside of the object. This is followed by a mesh refinement step. Following the above procedure, the total number of mesh elements was around 1.1–1.3 million cells for each hull design chosen for calculation. Sample results of discretization are shown in Figures 3 and 4.

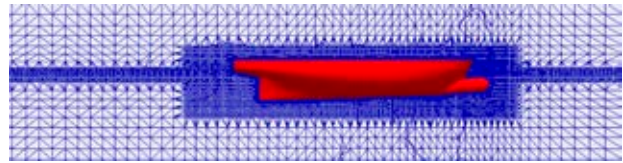


Figure 3. The side view example of a generated mesh. The denser grid was applied in the free surface region

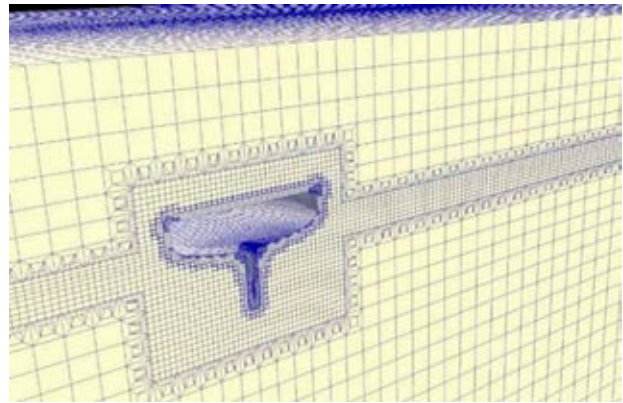


Figure 4. The cross view of a generated mesh. Hexagonal elements are present in the region where phase separation is supposed to occur

A numerical solution of flow is obtained on a grid covering only a selected area of an actual field flow (computational domain); therefore, it is necessary to introduce artificial boundary limits on the area and specific physical conditions on the surface of the hull, the free surface of the water, inlet, outlet and far field conditions were defined. The placement of the first grid point was chosen so as to keep the value of  $y^+$  below 200.

Due to the nature of the flow (high Froude number), an obvious first choice of modification, to

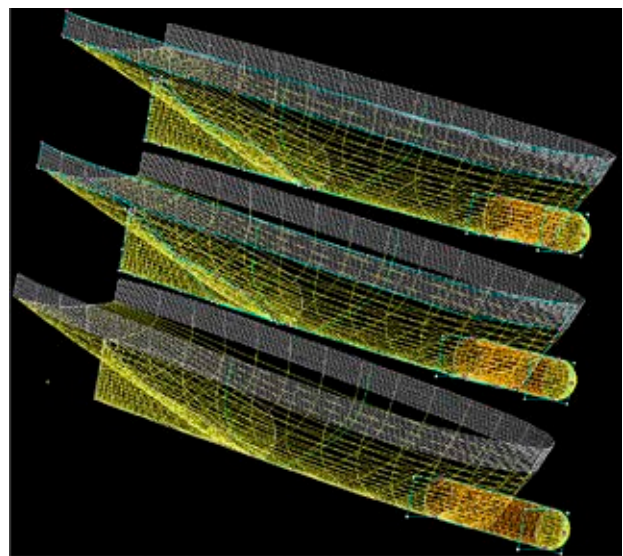


Figure 5. An example of developing shape modifications for testing – varying the length of a cylindrical bulb

improve the resistance characteristics of the hulls, is changing the shape of the bulbous bow. This approach is also justified by the fact that the proposed changes in shape are supposed to be applied to boats that are already in service, for which the possibility of changing global characteristics (i.e. length or breadth) are very limited.

Figure 5 presents one of several analyzed bulb shape applications and its systematic variation of length for testing. The impact of a “ducktail” device was the subject of other investigations.

### Chosen calculation results

The models were tested numerically at 1:5 scale. For large and fast transport ships, such a scale cannot be achieved due to the limitations to the first grid point location arising from high local Reynolds numbers. In the presented case, such a scale was possible due to the nature of the vessels’ operation (small fishing boats) and relatively lower associated Reynolds number. As a result, a reduction of the number of elements of the grid was possible. Due to a small change in the dimensions between a model

and a full scale vessel, relatively good dynamic similarity gives rise to small errors when translating results from the model scale to the full scale. Translation calculations of resistance were carried out in accordance with the standard ITTC (International Towing Tank Conference) procedure.

Example results of calculations are provided below. They determine the impact of tested bulbs on the hull resistance and, consequently, the effective power requirement of a fishing vessel. In addition, the results of the ducktail device on B25 type boat resistance are presented. The results of calculations for the B410 series vessel, involving the testing of the effect of some bulbs on the resistance value, are shown in Table 3.

The lowest power value was obtained in the case of modification No. 2 (effective power reduction of 16%) and for the modification No. 1 (effective power reduction of 14%). Modification No. 2 included the application of a streamlined and smooth bulbous bow, whereas modification No. 1 included application of an elongated cylindrical bulb. Both modifications are suitable for use in practice; however, modification 2 requires greater investment (CAPEX).

**Table 3. Chosen results of calculations for B410 series vessel – application of a bulbous bow**

| Froude number, $F_n$ | 0.335                              | 0.367    | 0.335  | 0.367    | 0.335                 | 0.367    |
|----------------------|------------------------------------|----------|--|----------|-----------------------|----------|
| Speed                | 2.3 m/s                            | 2.53 m/s | 10 knots   | 11 knots | 10 knots              | 11 knots |
|                      | Total resistance, model scale, [N] |          | Total resistance, full scale, ITTC procedure, [kN] |          | Effective power, [kW] |          |
| Basic hull           | 272.2                              | 363.4    | 33.6   | 45.1     | 172.6                 | 254.8    |
| Modification No.1    | 226.5                              | 310.8    | 27.8   | 38.3     | 142.7                 | 216.7    |
| Modification No.2    | 226.7                              | 304.3    | 28.1   | 37.9     | 144.5                 | 214.2    |

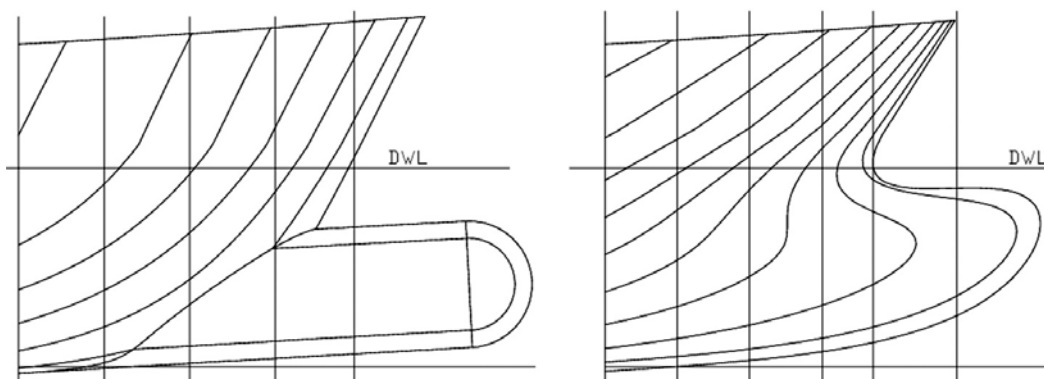


**Figure 6. Modifications to bulbous bow; left: modification No. 1, right: modification No. 2**

**Table 4. Chosen results of calculations for B25 series vessel – ducktail application**

|  | Basic hull | Ducktail application | Absolute difference | Relative reduction [%] |
|--|------------|----------------------|---------------------|------------------------|
| Total resistance, model scale, $V_m = 1.84$ m/s, [N] | 82.0       | 74.4                 | 7.59                | 9.26%                  |
| Total resistance, full scale, speed 8 knots, [kN]    | 10.13      | 9.21                 | 0.914               | 9.03%                  |

The shapes of the proposed changes are shown in Figure 6.

Table 4 shows the results from calculations on the hull of the B25 vessel with the application of a ducktail device. Reduction of the total resistance at full scale was equal to 9.03%. Given the analogous nature of flow for all vessels studied, there is justification to seek the potential use of this device in all similar vessels as similar flow effects may occur.

The ducktail device (Figure 7) extends the length of the waterline of a ship without significantly

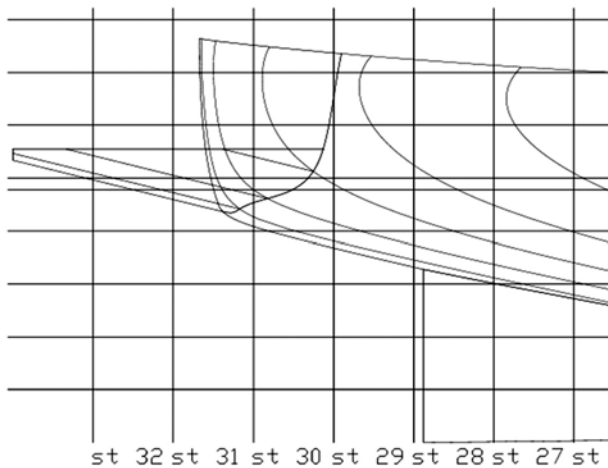


Figure 7. The ducktail device applied to B25 series vessel

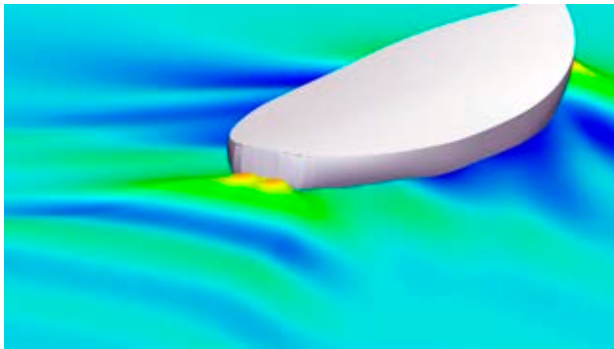


Figure 8. Wave system in the wake of B25 series boat without the ducktail device,  $L_{WLm} = 4.8$  m,  $F_n = 0.267$

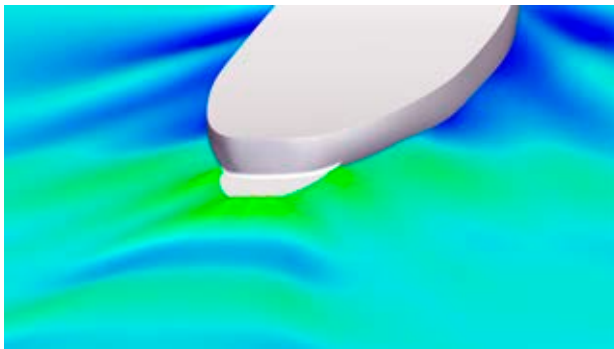


Figure 9. Wave system in the wake of B25 series boat with the ducktail device,  $L_{WLm} = 5.03$  m,  $F_n = 0.261$

increasing the wetted area of the hull or its weight. This element is mounted to the boat transom, directly on the waterline, mimicking the shape of the hull at the transom.

Since it extends the length of the waterline, the Froude number is reduced and the intensity of the wave system in the boat's wake is suppressed. The effect of the device is shown in Figure 8 (flow without the ducktail) and Figure 9 which show the wave system behind the stern without and with the device fitted. The suppression of wave height can be observed.

### Results generalization example and geometry parameterization

Due to the similar nature of the flow of the wave systems for all boats studied, it is possible to generalize the results by preparing proposals for the parameterization of the geometry of bulbous bows for design purposes. For example, the geometrical parameterization of a streamlined bulbous bow is given in Figure 10. The shape is defined by the coordinates  $x_1, x_2, x_3, x_4, x_5, x_6$  in the reference system with the origin located at the intersection of the design waterline and its perpendicular raised from the foremost point of the bow. The positions of these points are described by the coordinates where the variables denoted  $l_i$  refer to the length,  $t_i$  to the draught and  $b_i$  to the breadth. Their dimensionless values relate to the corresponding dimensions of the vessel under consideration. The values are shown in Table 5.

The geometry of the bulbous bow can be calculated for a given vessel by multiplying the relative value (Table 5) by its corresponding dimension (Table 1) of the main hull. E.g., in order to calculate the value  $l_1$  for the B280 fishing vessel:  $l_1 = 0.087$ , therefore  $L_{pp} = 0.087 \cdot 23.5 = 2.05$  m. In order to determine the values of  $t_i$  and  $b_i$ , the draught and breadth are used.

### Conclusions

The presented procedure and examples of calculation results show that the proposals for modifications to the shape of the hulls have the potential to decrease the impact on aquatic ecosystems by reducing the associated propulsion power; consequently, this will reduce a vessel's fuel consumption as well as the emissions of exhaust gases and CO<sub>2</sub>. Based on calculations for one B410 series fishing vessel, a generalized set of design variables was formulated that allows for the calculation of streamlined

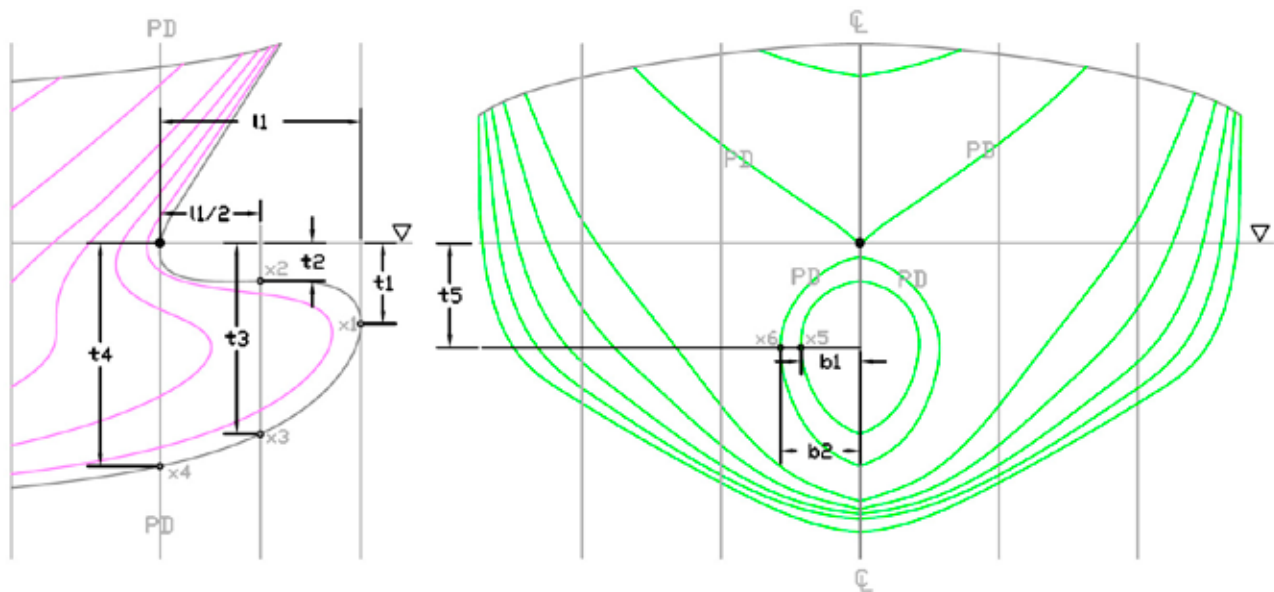


Figure 10. Values describing the location of the points  $x_1, x_2, x_3, x_4, x_5, x_6$  defining the shape of the streamlined bulbous bow. Variables denoted  $l_i$  refer to the length,  $t_i$  to the draught and  $b_i$  to the breadth. The origin is located at the intersection of the design waterline and its perpendicular raised from the foremost point of the bow

Table 5. Bulbous bow geometry parameterization for all fishing vessels

| General relative value,<br>defined according to Figure 10 [-] | K15<br>[m] | STOREM4<br>[m] | B25<br>[m] | KB21<br>[m] | B403, B410<br>[m] | B280<br>[m] | B275<br>[m] | B368<br>[m] |
|---|------------|----------------|------------|-------------|-------------------|-------------|-------------|-------------|
| $l_1$   | 0.087      | 1.47           | 1.41       | 1.90        | 1.65              | 2.00        | 2.04        | 1.30        |
| $t_1$   | 0.296      | 0.59           | 0.74       | 0.68        | 0.65              | 0.80        | 0.89        | 0.59        |
| $t_2$   | 0.141      | 0.28           | 0.35       | 0.32        | 0.31              | 0.38        | 0.42        | 0.28        |
| $t_3$   | 0.700      | 1.40           | 1.75       | 1.61        | 1.54              | 1.89        | 2.10        | 1.40        |
| $t_4$   | 0.815      | 1.63           | 2.04       | 1.87        | 1.79              | 2.20        | 2.44        | 1.63        |
| $t_5$   | 0.370      | 0.74           | 0.93       | 0.85        | 0.81              | 1.00        | 1.11        | 0.74        |
| $b_1$   | 0.081      | 0.40           | 0.43       | 0.53        | 0.53              | 0.58        | 0.60        | 0.42        |
| $b_2$   | 0.110      | 0.55           | 0.58       | 0.72        | 0.72              | 0.79        | 0.81        | 0.57        |

bulbous bow geometries for multiple hull designs. The *OpenFoam* system used for calculations could be used for further systematic shape optimization of the hulls of fishing vessels.

The proposed designs will be of greater significance in situations where fishery areas are more distant from ports and fishing vessels need to operate and transfer at full speed. Both proposed designs (ducktail and streamlined bulbous bow) reduce the wave component of the total resistance – an obvious focus of the optimization due to the intensive wave flows (all vessels have Froude number above 0.3).

An accurate economic assessment of the use of one of the presented designs should be left to a vessel's owner, who will have the best knowledge on the conditions under which the vessel is operated and who can better assess the relevance of the application of one of the proposed modifications. Further research to develop a methodology for such

an assessment, based on economic indicators such as internal rate of return, net present value and payback period of the invested capital, is planned.

A ducktail device may only be used on vessels that carry out fishing operations and release their fishing gear from their sides. The operation of this device is based on extending the length of the waterline of the ship without increasing the wetted area and suppressing the wave system in a vessel's wake.

## References

1. ABRAMOWSKI, T. (2005) Prediction of Propeller Forces during Ship Maneuvering. *Journal of Theoretical and Applied Mechanics* 43, 1. pp. 157–178.
2. ABRAMOWSKI, T. (2013) Application of Artificial Intelligence Methods to Preliminary Design of Ships and Ship Performance Optimization. *Naval Engineers Journal* 125(3). pp. 101–112.

3. ABRAMOWSKI, T., SZELANGIEWICZ, T. & ŻELAZNY, K. (2010) Numerical Analysis of Effect of Asymmetric Stern of Ship on its Screw Propeller Efficiency. *Polish Maritime Research* 4 (67), 17. pp. 13–16.
4. BERTRAM, V. (2000) *Practical Ship Hydrodynamics*. Butterworth-Heinemann.
5. BLADY, W. (2002) *Polska flota rybacka w latach 1921–2001*. Morski Instytut Rybacki.
6. CEPOWSKI, T. (2009) On the modeling of car passenger ferry ship design parameters with respect to selected seakeeping qualities and additional resistance in waves. *Polish Maritime Research* 3(61). pp. 3–10.
7. CEPOWSKI, T. (2010) Design Guidelines for Predicting Wave Resistance of Ro-Ro Ferries at the Initial Designing Stage. *Scientific Journal of the Maritime University of Szczecin* 22 (94). pp. 5–9.
8. FOLTYN, Z. (1978) Trawler rufowy typu B 410. *Budownictwo Okrętowe* 10–11.
9. FYSON, J. (Ed.) (1985) *Design of Small Fishing Vessels*. UN FAO.
10. GULBRANDSEN, O. (2012) *Fuel savings for small fishing vessels*. A manual, UN FAO.
11. JACQUIN, E., ALESSANDRINI, B., BELLEVRE, D. & CORDIER, S. (2002) *Yacht Optimisation Based on Genetic Algorithm and RANSE Solver*. HP Yacht Design Conf., Auckland, pp. 197–204.
12. OpenCFD Ltd ESI Group (2016) *Open Foam User Guide*. [Online] Available from: <http://openfoam.com/documentation/user-guide/> [Accessed: January, 2017]
13. PERI, D., ROSSETTI, M. & CAMPANA, E.F. (2001) Design Optimization of Ship Hulls via CFD Techniques. *Journal of Ship Research* 45/2. pp. 140–149.
14. PEYRET, R. & TAYLOR, D.T. (1983) *Computational Methods for Fluid Flow*. Springer-Verlag.
15. SZELANGIEWICZ, T., ABRAMOWSKI, T. & ŻELAZNY, K. (2010) Numerical Analysis of Influence of Ship Hull Form Modification on Ship Resistance and Propulsion Characteristics (Part III). *Polish Maritime Research* 1 (63), 17. pp. 10–14.